Mechanisms of Chlorophyllin Anticarcinogenesis against Aflatoxin B1: Complex Formation with the Carcinogen

ARTICLE *in* CHEMICAL RESEARCH IN TOXICOLOGY · JULY 1995

Impact Factor: 3.53 · DOI: 10.1021/tx00046a004 · Source: PubMed

4 AUTHORS, INCLUDING:

Roderick Dashwood
Texas A&M University System Health Science …

206 PUBLICATIONS **7,706** CITATIONS

Mechanisms of Chlorophyllin Anticarcinogenesis against Aflatoxin B_1: Complex Formation with the Carcinogen

Vibeke Breinholt,[†] Michael Schimerlik,[‡] Roderick Dashwood,[§] and George Bailey*,[†]

Department of Food Science and Technology, Graduate Program in Toxicology, and Department of Biochemistry and Biophysics, Oregon State University, Corvallis, Oregon 97331, and Department of Environmental Biochemistry, University of Hawaii, Honolulu, Hawaii 96822

Received October 3, 1994[⊗]

Chlorophyllin (CHL), a food-grade derivative of the green plant pigment chlorophyll, has recently been shown in this laboratory to be a potent inhibitor in vivo of hepatic aflatoxin B_1 (AFB_1)–DNA adduction and hepatocarcinogenesis (Breinholt et al. (1995) *Cancer Res.* **55**, 57–62). We report here that CHL forms a strong noncovalent complex with AFB_1 in vitro (dissociation constant (K_d) by Scatchard analysis = 1.4 (±0.4) μM based on copper chlorin content), which may contribute to its anticarcinogenic activity. K_d values for the related porphyrins chlorine e6, protoporphyrin IX, and zinc protoporphyrin IX were also of the same order of magnitude as that of the commercial CHL. Mole ratio analysis provided evidence that all porphyrins examined associate with AFB_1 at an approximate one to one stoichiometric ratio. Energy minimization computer modeling of the complex indicates a favorable association energy of −20 kcal/mol, independent of oxidation state of the 8,9-double bond of AFB_1. AFB_1 incubated in vitro with liver microsomes in the presence of added CHL showed comparable levels of inhibition in the production of several phase 1 metabolites, including the postulated procarcinogenic metabolite AFB1 8,9-epoxide. Kinetic analysis of microsome-catalyzed AFB_1–DNA adduction suggested a CHL inhibition constant near 10 μM chlorin. In vivo, addition of CHL to concentrated AFB_1 solutions followed by gavage administration resulted in dose-dependent inhibition of hepatic AFB_1–DNA adduction, whereas the same dosages of AFB_1 and CHL incorporated into a single bolus of trout diet for gavage provided less protection at all CHL doses. This observation demonstrates that prior or prolonged CHL treatment is not required for its antigenotoxic activity in vivo, but suggests that the efficiency of CHL protection may depend on sample formulation. These findings support a role for CHL–AFB_1 complex formation in CHL anticarcinogenesis. Since the CHL precursor chlorophyll is present at very high concentration in certain green vegetables such as spinach, complex formation between CHL-like compounds and carcinogens having at least partially planar aromatic structure may contribute to the chemopreventive activities associated with a high green vegetable intake.

Introduction

Intense recent research activity has led to the discovery of hundreds of chemopreventive agents, belonging to a very diverse class of chemicals, that are capable of interfering with key initiation or post-initiation processes in experimental carcinogenesis (*1–3*). Many of these agents are natural constituents of fruit and vegetables and have exhibited anticarcinogenic activity experimentally against a wide range of chemical carcinogens. Unfortunately, anticarcinogenic phytochemicals often occur individually in edible plants at relatively low concentrations, such that the doses required to elicit a chemoprotective effect in experimental animals often considerably exceed the amounts humans might encounter in a balanced diet. A promising exception is chlorophyll, the ubiquitous pigment abundant in green and leafy vegetables commonly consumed by humans. Recent studies have shown that chlorophyllin (Figure 1), a food-grade derivative and structural analogue of chlorophyll, strongly inhibits aflatoxin B_1 (AFB_1)–DNA damage (*4*) and hepatocarcinogenesis (*5*) in the rainbow trout model. In the trout model, over 70% inhibition of tumorigenesis was reached at an effective dietary chlorophyllin (CHL)[1] concentration of 0.14%, a fraction of the chlorophyll

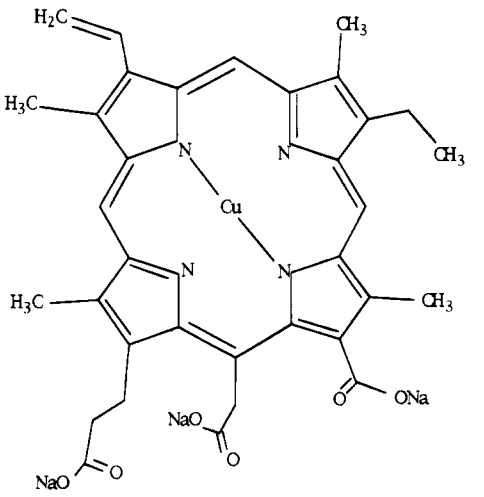

Figure 1. Structure of copper chlorophyllin, sodium salt.

* To whom all correspondence should be addressed. Phone (503) 737-3164, FAX (503) 737-1877.
[†] Department of Food Science and Technology, Oregon State University.
[‡] Department of Biochemistry and Biophysics, Oregon State University.
[§] University of Hawaii.
[⊗] Abstract published in *Advance ACS Abstracts*, April 1, 1995.

0893-228x/95/2708-0506$09.00/0

content of typical spinach isolates (2.6–5.7% dry weight) (*6*, *7*).

These findings may be taken to suggest that a nutritionally realistic intake of chlorophyll has the potential of exerting chemopreventive activities in humans against dietary and environmental carcinogens. However, the mechanisms responsible for CHL anticarcinogenesis and its potential for human chemoprevention are not yet clearly understood. Recent studies have shown CHL and related porphyrins to be capable of forming strong noncovalent complexes in vitro with genotoxins that have at least partially planar, aromatic character (*8–14*). Complexation between CHL and 2-amino-3-methylimidazo[4,5-*f*]quinoline (IQ) in the diet or digestive tract has been suggested to provide a less-absorbable complex responsible for reduced carcinogen bioavailability and target organ DNA adduction in vivo in rats (*15*). In addition, any CHL taken up systemically may complex in situ with procarcinogens to reduce the rate of enzymatic activation, or interact with electrophilic metabolites to directly interfere with DNA adduction.

Although a CHL antigenotoxic mechanism involving strong complex formation is suspected to be important only for mutagens or carcinogens that are at least partially aromatic and planar, these properties in fact are shared by numerous polycyclic aromatic hydrocarbons, heterocyclic amines, mycotoxins, and other suspected human carcinogens. Among these, AFB_1 is the most potent hepatocarcinogen known and the only naturally occurring compound in the human food chain concluded by the International Agency for Cancer Research (IARC) to be carcinogenic to humans (*16*). The purpose of the present study was to examine the strength and stoichiometry of molecular complexation between AFB1 and CHL in vitro and its relevance to CHL inhibition of AFB_1 metabolism and hepatocarcinogenesis in vivo.

Experimental Procedures

Materials. Unlabeled AFB_1 was purchased from Sigma Chemical Co. (St. Louis, MO), and the tritiated form from Moravek Biochemicals Inc. (Brea, CA). The purity of both preparations was determined by TLC and UV spectrophotometry. Calf thymus DNA, NADPH, proteinase K, RNase A and T1, and CHL were obtained from Sigma Chemical Co. The purity of the CHL preparation was analyzed by TLC as described (*17*). The preparation was found to resolve on TLC into at least 9 different chromophores, with two major fractions accounting for approximately 90% of the total pigment content as determined by preparative TLC (data not shown). These two major fractions corresponded in R_f values to copper isochlorin e4 and copper chlorin e6 (Ce6) identified by Sato et al. (*17*). Comparison of the TLC chromatogram of the Sigma CHL with that of a pure preparation of Ce6 (kindly provided by Dr. Hikoya Hayatsu) indicated that the specific lot of Sigma CHL used in these experiments was 35% total chlorins (range 33.5–36.8%). This is consistent with a copper content of 3.0 ± 0.2% (equivalent to 33.6 ± 2.4% total chlorins, MW 722) determined by atomic absorption spectrometry, and the supplier's claim that all copper in the preparation is porphyrin associated. A CHL chlorin value of 34% was used in this study to correct for nonchlorins in the CHL preparation. The remaining constituents of the Sigma CHL sample were, according to the supplier, inorganic salts including NaCl. Protoporphyrin IX (PP) and Zn-protoporphyrin IX (ZnPP) were obtained from Aldrich Chemical Co. (Milwaukee, WI). The purities of these compounds were determined spectrophotometrically to be approximately 94% (PP) and 99% (ZnPP).

Solvents used for HPLC analysis of AFB_1 metabolites were of HPLC grade, filtered through 0.2 μm pore size filter paper (Waters Associates) prior to use. Ultrapure phenol was from Clontech Laboratories Inc. (Palo Alto, CA). Aflatoxin standards were isolated and purified in our laboratory by HPLC; those used in the current study were AFB_1, aflatoxin M_1 (AFM_1), aflatoxicol (AFL), aflatoxicol M_1 (AFL-M_1), and aflatoxin B_1–glutathione conjugate. Aflatoxins are known to be potent hepatocarcinogens, and precautions must be taken to avoid human exposure or environmental contamination. All aflatoxin-containing solutions and glassware were decontaminated by 24 h treatment with bleach and Oakite detergent.

Methods. (A) Estimation of AFB_1–CHL Complex Formation. Complex formation between CHL and AFB_1 was studied fluorometrically by measuring the degree of quenching of the emission spectrum of AFB_1 by CHL. A photon-counting spectrofluorometer (SLM 8000) equipped with a 450W xenon lamp was used for the flourescence determinations, with a 365 nm wavelength for AFB_1 excitation. Experiments were conducted in 1 cm path length stirred quartz cuvettes maintained by thermoelement monitoring at 25 °C. The total volume of buffer (0.1 M Tris HCl, pH 7.4) before titration was 3 mL which included 10 μL of AFB_1 in 95% ethanol to a final concentration of 10 μM. After scanning the control AFB_1 spectrum and noting the total photon count at the given excitation and emission wavelengths, increments of 2 μL of CHL stock solution in the appropiate buffer were added to provide 2 μM final concentration increments, followed by remeasuring of the emission peak. Three to five separate titrations were conducted at each pH value up to a total of 50 μM added CHL. All CHL solutions were made up in amber microcentrifuge tubes to protect the compound from light. In order to determine the presence of an isosbestic point, complete emission spectra at several CHL concentrations at pH 7.4 were recorded at wavelengths between 360 and 580 nm. Dilution effects during these incremental additions were found to be negligible.

A similar set of analyses was conducted using 50 μM Na_2PO_4 buffers at pH 3.0, 4.5, 7.4, or 8.0 to examine the effect of pH on AFB_1–CHL complex formation. These pH values were chosen to encompass those measured within the rainbow trout digestive tract (stomach at fast: pH 2.5–3.0, stomach containing food: pH 4.5–6.8, pyloric stomach: pH 6.8–7.0, intestine: pH 7.2–7.6, cecum: pH 8.0).

(B) Determination of Complex Dissociation Constants. Dissociation constants (K_d) were established at 25 °C for the complex between AFB_1 and four selected porphyrin compounds: CHL, PP, ZnPP, and Ce6. The K_d for CHL and AFB_1 was also determined at three additional temperatures: 12, 37, and 55 °C. This set of titrations was conducted as described above, with a constant AFB1 concentration of 5.5 μM in 3.0 mL of 0.1 M Tris (pH 7.4) and successsive additions of 5.0 μL aliquots of porphyrin stock solutions. CHL and Ce6 were dissolved in Tris buffer (pH 7.4), and increments of 2 μM were added to the cuvette. Due to the low solubility of PP and ZnPP in solutes compatible with the fluorescence measurements, both compounds were ground into a fine powder and partly dissolved in 100% ethanol. The undissolved particles were sedimented by centrifugation, and the supernatant was transferred to a new amber micocentrifuge tube. The actual concentrations of PP and ZnPP in the supernatants were determined from absorbances of aliquots diluted into 1 M HCl (PP, E_{406} = 262 M^{-1} cm^{-1}) or pyridine (ZnPP, E_{425} = 146 M^{-1} cm^{-1}). The final concentrations of PP and ZnPP used for each addition were 1.4 and 1.0 μM, after additions of 2.0 and 2.5 μL, respectively. For Scatchard analyses, the concentration of free AFB_1 (AF_f) was calculated as:

[1] Abbreviations: aflatoxin B_1, AFB_1; aflatoxin M_1, AFM_1; aflatoxicol, AFL; aflatoxicol M_1, $AFLM_1$; acetonitrile/methanol/tetrahydrofuran, AMT; butylated hydroxyanisole, BHA; chlorin e6, Ce6; chlorophyllin, CHL; dimethyl sulfoxide, DMSO; 2-amino-3-methylimidazo[4,5-*f*]-quinoline, IQ; International Agency for Cancer Research, IARC; protoporphyrin IX, PP; zinc protoporphyrin IX, ZnPP.

$$AF_f = (AF_i)(FCHL_x/FAF_i)$$

where AF_i is the initial concentration of AFB_1 (μM), FAF_i the concomitant fluorescence yield, and $FCHL_x$ the photon count after adding x μM CHL to the cuvette. The concentration of bound AFB_1 (AFb) and of bound CHL (CHLb) was calculated as:

$$AF_b = CHL_b = AF_i - AF_f$$

where AF_f is the concentration of free substrate. The concentration of free ligand (CHL_f) was determined as the difference between the total concentration of CHL added to the cuvette (CHL_x) and CHL_b, i.e.:

$$CHL_f = CHL_x - CHL_b$$

Plots of (CHL_b/CHL_f) against CHL_b were modeled as linear data sets, with slopes describing the negative reciprocal dissociation constant ($-1/K_d$) and the x-intercept the concentration of CHL at complex saturation. The value of this intercept divided by the initial concentration of AFB_1 provides one measure of the mole ratio of the CHL–AFB_1 complex at CHL saturation.

(C) Mole-Ratio Determinations of the AFB_1–CHL Complex. The presence of a defined complex mole ratio between AFB_1 and CHL was also evaluated using a similar approach except that the initial AFB_1 concentration was 50 μM, and CHL was added in increments of 2 μM. A reverse titration also was conducted in which CHL in excess (50 μM) was titrated with 5 μM aliquots of AFB_1 contained in 5 μL of dimethyl sulfoxide (DMSO). Changes in AFB_1 fluorescence were measured at 440 nm. Due to the relatively low water solubility of AFB_1 a 33% DMSO–Tris buffer (pH 7.4) was employed for this set of experiments, with the realization that K_d values in this solvent may differ from those in an entirely hydrophilic (or hydrophobic) environment.

(D) Molecular Modeling. Initial structures of AFB_1 and CHL were constructed using MM2 force field parameters and conjugate gradient methods. Complexes were minimized to a gradient of 0.001 kcal/mol, and calculations were performed using HyperChem Release 2 (Autodesk) on an IBM 486-based PC. The free base derivative of CHL was used since previous studies have shown that the 4-coordinate central copper atom does not influence π–π interactions and complex formation (*18*, *19*). Complexes were obtained by first energy minimizing the structures of CHL and AFB_1 separately, and then placing AFB_1 and CHL within van der Waals radii and energy minimizing the corresponding complex.

(E) AFB_1 Metabolism by Microsomes in Vitro. Trout liver microsomes were prepared as described (*20*), resuspended in ice cold 0.1 M potassium phosphate (pH 7.5), 30% glycerol, and 1 mM EDTA, and stored in 0.5 mL aliquots at −80 °C until use. Protein concentations were determined by the method of Lowry et al. (*21*).

The in vitro DNA adduction reaction mixture consisted of 1 mg of calf thymus DNA, 0.5 mg of microsomal protein, and AFB_1 at concentrations between 5 and 50 μM dissolved in 10 μL of DMSO (0.86 μCi/sample). CHL dissolved in reaction buffer was added to a final concentration of 0, 10, 25, 50, or 150 μM. Each incubation in triplicate was made up to a total volume of 1.0 mL with a 50 μM Na_2PO_4 buffer (pH 7.4), containing 100 μM EDTA and 1.5 mM $MgCl_2$. After vortexing and 2–3 min preincubation, the reaction was initiated with 5 μM NADPH and allowed to proceed for 15 min at 25 °C in the dark. During this time period DNA adduction occurred in a linear fashion (data not shown). The reaction was terminated by addition of 100 μL of 10% SDS and 9 units of proteinase K dissolved in 50 μL of reaction buffer. The samples were then incubated at 55 °C for 30 min and cooled to room temperature. DNA was purified and assayed by the Burton method (*22*) and its specific activity determined as described (*23*).

Metabolism of AFB_1 in vitro was assessed by HPLC analysis as described by Monroe and Eaton (*24*) with modifications. Incubations were conducted in total volumes of 0.25 mL, and only one level of AFB_1 of 10 μM (5 μCi/sample) was employed, with and without addition of 100 μM CHL to the incubation mixture. The reaction mixture consisted of 6.0 mg of microsomal trout protein/mL and 12 mg of butylated hydroxyanisole (BHA)-induced mouse cytosolic protein/mL, in a buffer containing 190 mM sucrose, 60 mM potassium phosphate, 80 mM Tris, 15 mM NaCl, 5 mM KCl, and 4 mM $MgCl_2$ (pH 7.6). The mouse cytosolic fraction was isolated from Swiss-Webster mice fed a AIN-76A semipurified diet containing 0.75% BHA for 10 days. Reaction mixtures containing CHL and AFB_1 were preincubated for approximately 2 min before initiation of the reaction with 5 mM reduced glutathione (GSH) and 5 μM NADPH. Additional controls lacking GSH, mouse cytosol, or microsomes were included in order to distinguish between mouse cytosol-dependent metabolism and trout microsome-mediated activities and to verify the formation of the AFB_1–GSH conjugate. This method (*24*) provides exogenous glutathione transferase and GSH to quantify AFB_1-8,9-epoxide production by trapping as the conjugate. Reactions were terminated by addition of 1.0 mL of 100% methanol followed by high speed vortexing for 30 s. The denatured protein was centrifuged at 14000*g* for 15 min. The supernatant was transferred to a microcentrifuge vial and frozen at −20 °C overnight. The frozen mixture was centrifuged at 14000*g* for 5 min at ambient temperature to allow thawing of the mixture and to precipitate remaining protein. Particulate matter was removed by filtration of the supernatant (0.2 μm syringe filter, Waters Associates) into a 2 mL sonicated glass vial. The methanol was evaporated under a stream of nitrogen and the sample adjusted to 15% AMT (acetonitrile/methanol/tetrahydrofuran (15:20:6)) and 85% 0.02 M potassium acetate (pH 5.0) immediately prior to HPLC. A total of 50 μL in duplicates was injected per incubation, with triplicate incubations carried out.

Analysis of AFB_1 metabolites was performed with a Beckman 110B solvent delivery module connected to a 421A controller unit and a programmable absorbance detector, Spectroflow 783 (Kratos Analytical). The metabolites were separated on a 25 cm × 4.7 mm i.d. Spherex C_{18} column (Phenomenex). A 50 μL precolumn (Upchurch Scientific, Oak Harbor, WA) packed with C_{18} Corasil supported by 0.5 μm frits was used to protect the analytical column and to remove interferring components. AFB_1 and metabolites were eluted from the analytical columnn at 1 mL/min with 0.02 M potassium acetate (pH 5.0) and AMT (20:15:6) run in a linear gradient of AMT from 15% to 46% over a period of 30 min. Between 60 and 100 fractions of 200 μL were collected per injection. Metabolites were identified on the basis of retention times of external and internal standards.

(F) In Vivo AFB_1–DNA Binding. Ten groups of 9 rainbow trout of 15–20 g body weight were placed in separate tanks and fasted for 7 days, to obtain complete emptying of the digestive system. At the end of this period one group of fish received 6.6 ng (0.3 μCi) of tritiated AFB_1/15 g body weight by gavage using 10 μL of 0.9% NaCl as a carrier. This amount of AFB_1 is equivalent with a 20 ppb daily dietary dose, when the dietary ration (dry weight) is fed daily at 2% of the body weight. Four other groups received the same dose of AFB_1 in combination with CHL concentrations of 0.03, 0.16, 0.66, and 1.31 mg, equal to CHL dietary levels of 100, 500, 2000, and 4000 ppm. All solutions were made up in 0.9% NaCl.

The remaining fish received the same doses of AFB_1, or AFB_1 plus CHL, incorporated into a modified Oregon Test Diet mixture consisting of 28% dry ingredients (20% salmon oil, 40% casein, 15% α-cellulose, 9% gelatin, 8% dextrin, 4% essential minerals, 2% vitamin mix, 1% choline chloride, and vitamin E (660 IU/kg dry ingredients)) and 72% water. The water content of the gavaged diet was slightly increased over the 65% normally used in feeding trials in order to increase fluidity for gavage administration of the food bolus. Each fish was given a total of 140 mg (wet weight) diet mixture/15 g body weight. The same solutions of AFB_1 and CHL used in the liquid gavage experiment were used for making up the gavage diet, to a total water content of 72%. Forty-eight hours after administration of

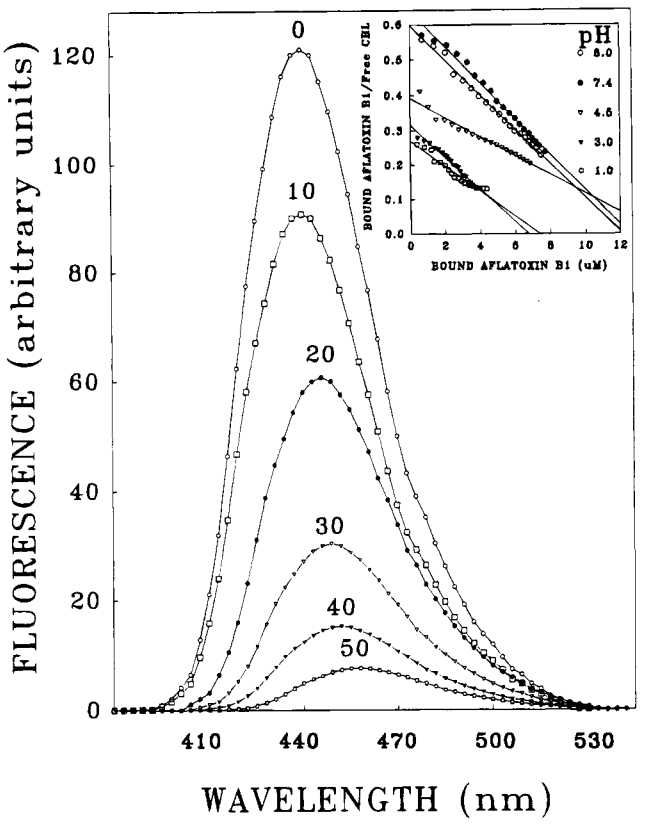

Figure 2. Quenching of AFB_1 fluorescence spectrum by CHL. AFB_1 at a final concentration of 10 μM was titrated with 10 μM aliquots of CHL. Number 0 is the control fluorescence curve of AFB_1. Numbers represent the fluorescence yield after addition of 0, 10, 20, 30, 40, and 50 μM CHL. Inset: Scatchard plots of AFB_1-quenching curves at pH 7.4 (filled circles), pH 8.0 (open circles), pH 4.5 (open triangles), pH 3.0 (filled triangles), and pH 1.0 (open squares).

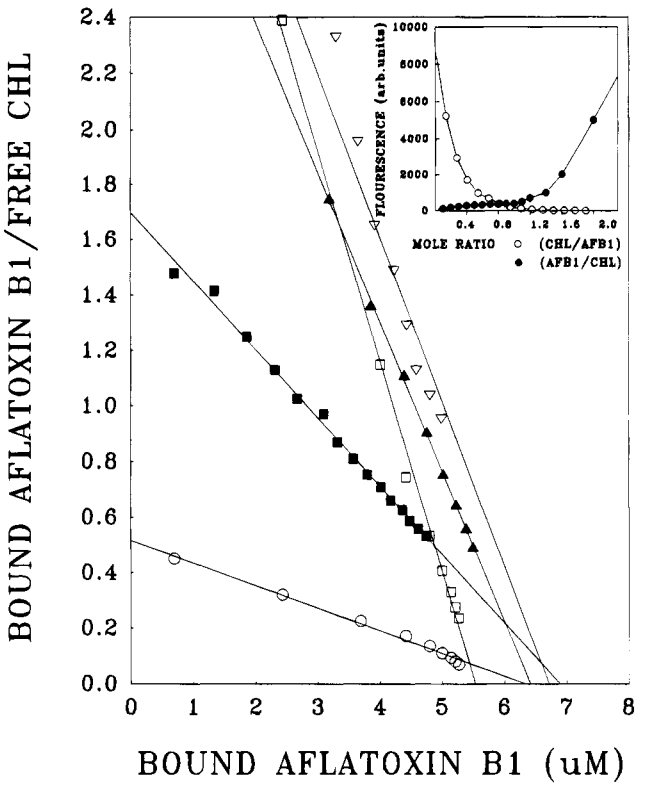

Figure 3. Scatchard plot of AFB_1 fluorescence quenching data. The data points are mean values of 3–6 individual determinations; error bars are omitted for clarity. Open circles: CHL (without correction for impurities); open squares: CHL (corrected for specific pigment content); filled triangles: pure copper chlorin (Ce6); open triangles: ZincPP; filled squares: PP. Inset: Mole ratio analysis. The open circles represent the general form of the titration curve obtained by quenching AFB_1 fluorescence with small aliquots of CHL. The filled circles are the reverse titration where CHL is kept constant upon addition of increasing amounts of AFB_1.

carcinogen and inhibitor, fish were killed by a blow to the head, livers were removed, and pools of three livers each were frozen in liquid nitrogen and stored at −80 °C until analysis. Liver DNA was isolated as described previously (*23*). The DNA pellet was dissolved in 1.0 mL of 10 mM Tris buffer overnight at 5 °C and the purity determined by measuring the 260/280 nm absorbance ratio (1.8–2.0 for all samples).

Results

CHL Quenching of the AFB_1 Fluorescence Spectrum. The ability of CHL and individual porphyrin analogues to quench the fluorescence spectrum of AFB_1 was used as a measurement of complex formation with AFB_1. Since the fluorescence optimum of CHL is near 700 nm and completely separated from the AFB_1 fluorescence peak, AFB_1 fluorometric measurements provide a very sensitive, though indirect, index of AFB_1–CHL interaction. Stopped-flow analysis revealed that AFB_1–CHL association in vitro was rapid and complete within the 2.5 ms required to mix the two components in the stopped-flow photometer (data not shown). The optimum fluorescence yield was linear with AFB_1 through the concentration range of this study (not shown), which indicates an absence of significant AFB_1–AFB_1 interaction under these conditions.

During the titration process AFB_1 fluorescence decreased and the optimum shifted to higher wavelengths in the presence of CHL (Figure 2). This indicates that the florescence characterictics of AFB_1 change due to the interaction between the two compounds. The degree of spectral shift was approximately 0.3 nm/μM CHL at pH 7.4. The noncovalent nature of the complex was verified by dilution of a solution containing AFB_1 and CHL at a 1:4 ratio, in which the AFB_1 maximum fluorescence peak had been shifted 22 nm upfield. Serial 1:1 dilutions resulted in successive increases in fluorescence yield despite the gradual decrease in total AFB_1 concentration in the cuvette, and reappearance of the characterictic 440 nm AFB_1 emission maximum (data not shown).

Determination of Complex Dissociation Constants. Figure 3 depicts Scatchard plots for the AFB_1–porphyrin complexes analyzed. The dissociation constants for complexes between AFB_1 and the four porphyrin compounds CHL, PP, ZnPP, and Ce6 were estimated by regression to be 1.4 (±0.4), 4.1 (±0.6), 1.6 (±0.3), and 1.9 (±0.5) μM, respectively. This K_d value for CHL is based on the actual concentration of CHL in the preparation (ca. 34%); without correction, the calculated K_d was 11.6 (±3.3) μM (Figure 2). A similar K_d value (data not shown) for the CHL–AFB_1 complex was obtained using spectrophotometric methods as described elsewhere (*10*). The x-intercepts of the Scatchard plots (Figure 2) define the concentration of ligand sufficient to saturate complex formation at the particular substrate concentration used and thus provide a measure of complex stoichiometry. None of the intercepts on the x-axis of the Scatchard plots for the four porphyrins were significantly different by analysis of variance ($p > 0.30$). The mean value of all replications from the individually repeated titrations was

found to be 6.1 (±1.5) μM. The presence of an isosbestic point obtained from the complete emission spectra (not shown), along with the finding that the x-intercept on the Scatchard plot (6.1 μM) approximates the AFB_1 concentration employed in this titration series (5.5 μM), confirms that AFB_1 and the porphyrins associate stoichiometrically at an approximate 1:1 ratio.

The stoichiometry between AFB_1 and CHL was also investigated as suggested by Christwell and Schilt (*25*), using an initial AFB_1 concentration approximately 35-fold higher than the AFB_1–CHL complex K_d, in order to seek an initial linear change in fluorescence. At the sensitivity of the fluorometer, 50 μM AFB_1 was the highest concentration which gave a linear response in AFB_1 fluorescence. The first series of experiments (forward titrations) were conducted by measuring the decrease in AFB_1 fluorescence with increasing CHL concentration. The forward titration should ideally result in an initial quenching of AFB_1 fluorescence spectrum in approximate proportion to the ligand added, until the substrate is maximally complexed. At this transition point, defining the mole ratio of the associating molecules, further addition of ligand will not result in changes in fluorescence. The reverse order of reaction (reverse titration) was also examined by determining the ability of a fixed concentration of CHL (in excess over K_d) to bind increasing amounts of AFB_1, such that AFB_1 flourescence emission is suppressed until the stoichiometry of complexation is exceeded.

A fluorescence transition was found to occur with tangents intersecting near a 1:1 mole ratio for the "reverse" titration (Figure 3, inset). However, the data display sigmoid rather than linear behavior near the origin, and a sharp break point characteristic of extremely tight complex associations (*25*) was not evident. The lack of a sharp break point might reflect the presence of several chlorins of widely different affinities for forming a complex with AFB_1, but this seems unlikely since the commercial CHL when corrected for chromophore content gave a K_d identical to that for the pure Ce6. For the "forward" titration of fixed AFB_1 with successive CHL additions, an even less definitive break was observed, and this transitional change occurred in the range more compatible with a stoichiometry of 2 AFB_1:CHL. An additional observation, for which we currently have no satisfactory explanation, is a greater than stoichiometric depression in fluorescence with the first CHL additions in the forward titration. That is, AFB_1 fluorescence decreased by about 40% with the addition of only an 0.2 mole ratio of CHL. The most obvious possibility for these two observations, that complex stoichiometry may vary according to input mole ratio (e.g., AFB_1:CHL:AFB_1 complexes at low CHL input), is not supported by the largely linear Scatchard data. However, the latter were conducted at much lower CHL and AFB_1 concentrations, and it is possible that some other form of ligand self-association alters the effective fluorescence suppression of the complex. It is interesting that the forward and reverse titration curves cross over at a 1:1 mole ratio, though we have devised no theoretical argument that this should provide the best estimate of complex stoichiometry. It should be emphasized that changes in AFB_1 fluorescence do not provide a direct measure of the amount of complex formed, so that this type of experiment can provide only an approximate measure of true complex stoichiometry. We also point out that other models, such as formation of higher molecular weight aggregates having 1:1 CHL:AFB_1 stoichiometry, may be equally compatible with our data and perhaps more consistent with the strong binding indicated by a K_d of 1.4 μM.

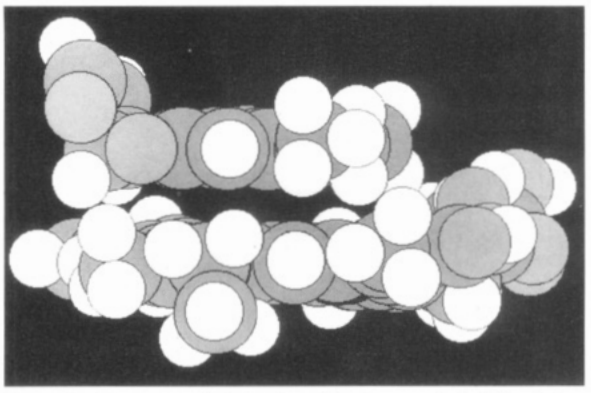

Figure 4. Energy-minimized molecular model of the interaction between AFB_1 (top structure) and CHL.

pH Effects on AFB_1–CHL Complex. Because of our interest in modeling the effects of dietary CHL chemoprevention, it was important to investigate whether pH variations along the digestive tract might influence complex stability or stoichiometry. On the basis of slopes of Scatchard plots (Figure 2, inset) derived from AFB_1 quenching experiments conducted at various pH values, the K_d for the AFB_1–CHL complex shows little dependence on pH. There was some evidence for a small (ca. 2-fold) effect at pH 4.5, which suggests some role for CHL carboxyl protonation on complex formation, but this was not sustained at lower pH. These results indicate that CHL–AFB_1 complex formation and stability in the acid conditions of the stomach are comparable to that expected elsewhere along the digestive tract.

Though K_d showed little sensitivity to pH change, the apparent intercept values decreased substantially at low pH. *A priori* this observation would suggest that complex stoichiometry is pH dependent. An alternative explanation is that this is an artifact of CHL self-interaction, which we have observed to increase at low pH, eventually to the point of CHL precipitation in unstirred solutions. An additional factor to be considered involves the potential for water addition across the AFB_1 8,9-double bond, a vinyl ether structure susceptible to acid-catalyzed hydrolysis (*26*). Hydrolysis would not be expected to influence K_d since this region is remote from the conjugated, planar portion of the AFB_1 molecule and hence is unlikely to be involved in CHL interaction (see modeling results). We do, however, observe substantial reduction in fluorescent yield when AFB_1 is incubated at low pH (not shown), which may be a result of hydrolysis. That the difference in y-axis intercepts from the Scatchard plots is not a result of increased AFB_1 self-quenching at low pH is evidenced by the fact that readjusting the pH of a solution at low pH back to pH 7.4 does not result in the expected fluorescence yield at this given pH, indicating that the fluorescence change is irreversible. Therefore, the data from this experiment support the conclusion that complex K_d is not strongly influenced by pH, but do not provide unambiguous information regarding possible pH effects on complex stoichiometry. Our interpretation is that stoichiometry is not pH dependent, since it is difficult to envision how this could occur without concomitant K_d effects.

Molecular Modeling. Figure 4 depicts one energy-

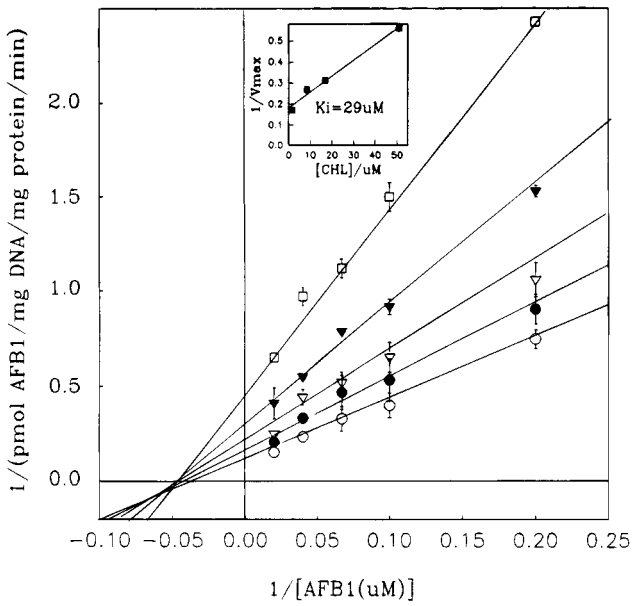

Figure 5. CHL inhibition of microsome-catalyzed AFB_1–DNA adduction in vitro. CHL was added at 0.0 (open circles), 5.0 (filled circles), 25 (open triangles), 50 (filled triangles), and 150 μM (open squares).

minimized structure for the CHL–AFB_1 complex based on computer modeling. Several different geometries were energy minimized, the most favored of which is shown here. The energy of the complex was −19.023 kcal/mol, with the 8,9-double bond of AFB_1 orientied 180° with respect to the carboxyl groups of CHL. Complex modeling between CHL and AFB_1, AFB_1-8,9-epoxide, and AFB_1-8,9-dihydrodiol all had similar minimization numbers (−16 to −21 kcal/mol), whether the 8,9-region was oriented toward or away from the CHL carboxyl groups. Clearly, the AFB_1 molecule has sufficient planarity and conjugation to form a strong 1:1 complex with CHL in the orientation shown. Since the furan ring containing the 8,9-double bond is nonplanar with the rest of the molecule, it is not expected that a complex having CHL:AFB_1:CHL stoichiometry would be preferred. We did not conduct energy-minimization calculations for the alternative AFB_1:CHL:AFB_1 trimolecular complex. We have previously shown that CHL interacts directly with the AFB_1-8,9-epoxide to depress its mutagenesis in the *Salmonella* assay (*4*), but have not determined if this involves CHL-mediated catalytic hydrolysis of the epoxide. The AFB_1–CHL orientation shown in Figure 4 seems unlikely to support direct CHL catalysis due to poor proximity of the 8,9-region and CHL.

CHL Effects on DNA Adduction and AFB_1 Metabolism in Vitro and in Vivo. We wished to determine if CHL might influence the rate of enzyme-catalyzed AFB_1 metabolism to DNA binding species, were CHL to accumulate to significant concentrations within target organ cells in vivo. AFB_1–DNA adduction was found to be strongly inhibited in the presence of increasing CHL concentration in the reaction mixture (Figure 5). As shown in the figure, intersection of individual lines fitted independently by linear regression suggests inhibition which has an appearance of being noncompetitive, with K_i values near 29 μM CHL or, in terms of true chlorin content, 10 μM. However, we stress that catalysis was carried out here using trout liver microsomes, which have

Table 1. Effect of CHL on the Percentage Distribution of AFB_1 and Its Phase 1 Metabolites after in Vitro Incubation with Trout Hepatic Microsomes

metabolite[a]	control	CHL (100 μM)	inhibition by CHL[b] (%)
AFB_1	90.7 (0.38)	95.2 (0.04)[c]	48
AFM_1	3.13 (0.0.25)	2.12 (0.19)[c]	32
AFL	2.24 (0.17)	0.99 (0.25)[c]	54
$AFLM_1$	1.60 (0.33)	0.88 (0.13)[c]	44
AFB_1 epoxide	2.34 (0.19)	0.75 (0.23)[c]	65
total metabolites	9.17 (0.29)	4.75 (0.29)	48

[a] Abbreviations: AFB_1, aflatoxin B1; AFM_1, aflatoxin M1; AFL, aflatoxicol; $AFLM_1$, aflatoxicol M1. The figures in columns 2 and 3 represent the relative percentage of each of the five compounds determined by HPLC. [b] For AFB_1, calculated as inhibition of parent compound metabolized, i.e., 100(1 − 4.8/9.2). For others, calculated as percent inhibition of metabolite formed, i.e., 100(1 − CHL/control). [c] Significantly different from control, $p \leq 0.05$. Values are means of three determinations (±SD). Results are representative of two independent experiments.

one major (*27*) and at least one minor[2] cytochrome P450 isoform that catalyze AFB_1-8,9-epoxidation. The individual contributions of these P450s and their catalytic constants are not yet known; hence a more formal kinetic modeling of the entire data set to determine inhibition mechanism and inhibition constants would be premature. The present result is compatible with CHL interaction with substrate as well as enzyme, as reported for CHL inhibition of rat liver ethoxyresorufin *O*-deethylase activity (*28*), but studies with purified enzyme are needed to substantiate this mechanism.

We also examined the effect of CHL on the profile of microsome-catalyzed phase 1 metabolites. The trout hepatic microsomes for this experiment displayed a moderate AFB_1 Michaelis constant near 30 μM and moderate catalytic capacity for AFB_1 metabolism. By using 10 μM high specific activity AFB_1, it was possible to maintain an acceptably linear, quantifiable reaction with reasonable levels of microsomes. These assays were thus designed to consume only about 10% of the added substrate in order to assure that AFB_1 was not depleted, to enable quantification of metabolites with ample precision, and to avoid the use of saturating substrate conditions which would have masked any partially inhibitory effect of CHL. As seen in Table 1, inclusion of a 10-fold molar excess of CHL reduced total microsome-catalyzed AFB_1 metabolism by about 50%, with significantly reduced production of all metabolites ($p < 0.05$) including the AFB_1-8,9-epoxide (trapped as glutathione conjugate). The data are consistent with an essentially uniform suppression of all AFB_1 metabolic reactions via CHL–AFB_1 complexation, but do not rule out the possibility that the results reflect similarly effective inhibition of several biotransforming enzymes by CHL.

The potential of increasing concentrations of CHL to inhibit AFB_1 binding to hepatic DNA in vivo was also examined, along with the influence of dietary components on inhibitory potency. As seen in Figure 6, inclusion of CHL at levels up to 4000 ppm in a liquid gavage provided dose-responsive inhibition of hepatic AFB_1–DNA adduction in vivo. Saturation of inhibition at about 80% appeared to be approached at the highest CHL concentration tested. Inclusion of the same AFB_1 and AFB_1 plus CHL doses incorporated into Oregon Test Diet formulation also provided dose-responsive CHL inhibition of

[2] N. Takahashi, D. E. Williams, and G. S. Bailey, unpublished results.

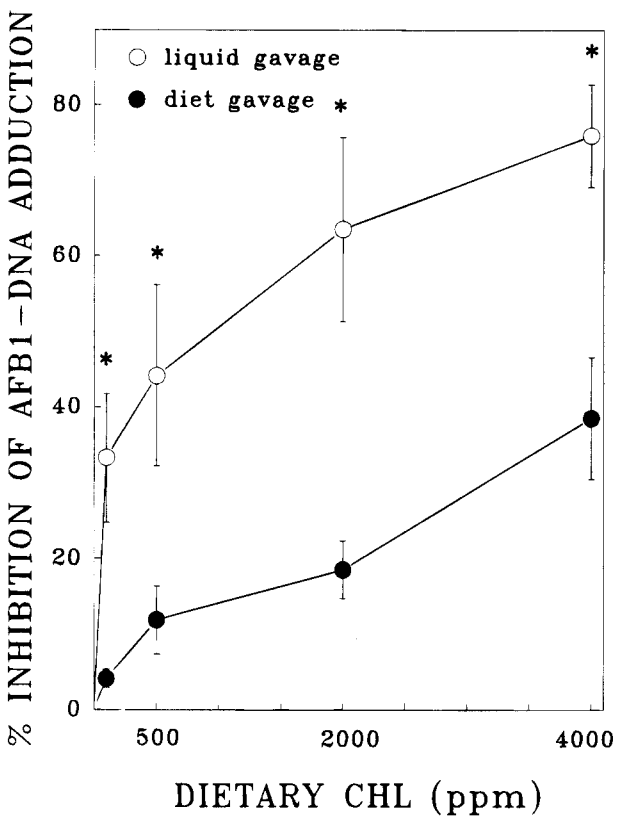

Figure 6. Enhanced inhibitory effect on in vivo AFB_1–DNA adduction by gavage administration of carcinogen and inhibitor in a small volume of saline at physiological pH, compared to administration by diet gavage of identical AFB_1 and CHL concentrations. *: $p < 0.05$ determined by analysis of variance.

AFB_1–DNA adduction. However, the liquid gavage of CHL in combination with AFB1 afforded significantly higher protection against AFB_1–DNA adduction than exposure via the diet, at each CHL level tested ($p \leq 0.05$).

Discussion

Dissociation Constant and Mole Ratio Determination. Complex formation has been suggested to be one of the main mechanisms responsible for the antimutagenic properties of CHL against many (*4*, *8*–*10*), but not all (*28*) mutagens of planar polycyclic ring structure. Other mechanisms such as enzyme inhibition (*29*–*32*), electrophile scavenging (*4*, *11*, *17*, *33*), inhibition of cell mitosis (*34*–*36*), and modifying effects on DNA-repair enzymes (*37*) also have been invoked to explain the antimutagenicity of CHL toward nonplanar, noncyclic genotoxins. Complex formation in the gastrointestinal tract between carcinogens and CHL has recently been suggested to explain CHL protection against carcinogen–DNA adduction in experimental animals in vivo (*4*, *15*), by reducing carcinogen absorption from the gut. In the present study the K_d for the 1:1 complex formed between AFB_1 and CHL (K_d = 1.4 μM) was found to be 2 orders of magnitude smaller than that reported for the complex between CHL and the heterocyclic amine IQ (K_d = 141 μM) assuming a 2:1 CHL:IQ stoichiometry (*15*). However, direct comparison of complex strengths is not possible since the true copper chlorin content of the CHL preparation used for the IQ studies was not specified. As with the IQ–CHL complex (*10*), the AFB_1–CHL complex dissociation constant was found not to vary substantially with pH, implying equivalent complex stability along the digestive tract. The K_d values for the various porphyrinic compounds were all in the same range, with PP showing a slightly weaker ($p < 0.05$) complexing ability than CHL, Ce6, and ZnPP.

Analysis of complex stoichiometry by reverse titration of CHL with added AFB1 provided some evidence for a 1:1 CHL:AFB_1 mole ratio. By comparison, the fixed concentration of AFB_1 for the forward titration was limited by AFB_1 solubility and may have been insufficiently in excess of the K_d (ideally 100-fold) to give a sharp break point indicative of a specific complex stoichiometry. Scatchard plots independently demonstrate an approximate 1:1 stoichiometry between CHL and AFB_1 and between AFB_1 and PP, ZnPP, and Ce6, based on extrapolated intercepts. This is in contrast to the 2:1 stoichiometry reported for CHL complexation with some heterocyclic amines (*10*), which may reflect the relatively asymmetric planarity of AFB_1 and a reduced ability to form symmetrical CHL:AFB_1:CHL structures. Another explanation for this discrepancy could be that no correction for the specific chlorin content was performed in the heterocyclic amine studies. If, for example, the CHL preparations used by Dashwood and Guo (*10*) were also 34% copper chlorins, replotting the mole ratio data gives a stoichiometry of 0.7:1 (CHL:IQ), similar to the CHL:AFB_1 mole ratio estimated here, and would result in a different calculated K_d value for this complex.

Correction for Specific Chromophore Content. Comparison of the K_d obtained from the pure copper Ce6 with that of the commercial CHL preparation might be taken to indicate a greater than 5-fold difference in the strength of the complexes. The K_d obtained for the pure copper chlorin was 1.9 μM whereas that of the commercial CHL was 11.1 μM (Figure 3). However, correction for the specific pigment content in the commercial sample gave a K_d of 1.4 μM, similar to that for the pure chlorin. As pure CHL is currently unavailable on a commercial scale, the finding that the complexing characteristics of the total individual fractions on a molar basis approximate that of a pure chlorin supports the use of commercial CHL for anticarcinogenesis studies against AFB_1. However, other carcinogens may not show uniform complexation among structurally variant porphyrins and chlorins.

Complex Formation as a Mechanism of Anticarcinogenesis. We have recently demonstrated that dietary CHL protected against AFB_1 carcinogenesis, but that this could be explained only partially by a complex formation mechanism (*5*). Quantitative comparisons of dose-related decreases in DNA adduct inhibition and in final tumor response revealed that the tumorigenesis protection afforded by doses of CHL at 2000 ppm or less could be accounted for by a decrease in AFB_1–DNA binding. This is compatible with the idea that complex formation in the digestive tract or target organ reduced AFB_1–DNA adduction and consequent tumorigenesis. However, at 4000 ppm CHL the reduced AFB_1–DNA adduction accounted for only 40–50% of the reduction in tumor response. It follows that some cellular mechanism(s) in addition to complex formation must contribute to the protective activity at higher CHL dose.

Further, complex formation characteristics in pure solution in vitro clearly overestimate the protective effect of CHL in vivo. As an example, the addition of 2000 ppm CHL (680 ppm actual chlorin content) to diets containing 20 ppb AFB_1 resulted in only 32% inhibition of AFB_1–DNA adduction in the target organ (*5*). This indicates

that about $^2/_3$ of the initial dietary AFB_1 dose in this tumor study remained bioavailable for absorption and bioactivation, despite a molar excess of CHL (43 000:1) sufficient to assume 100% complex formation with AFB_1 in solution in vitro. In the in vivo study reported here (Figure 6), complex formation was optimized by dissolving the reactants in a small volume of water and allowing the two compounds to interact prior to incorporation into the diet. However, the subsequent addition of water (72% of total diet) and dry ingredients reduced CHL protection, when compared to CHL effectiveness given with AFB_1 by liquid gavage. A reasonable interpretation is that diet formulation interferes with AFB_1–CHL complexation, both because the complex solution becomes diluted and because of the potential binding of AFB_1 or CHL to such constituents of the diet as the aromatic amino acids, vitamins, and cofactors exhibiting similar chemical structures. The extent to which porphyrinic compounds specifically encounter and bind dietary carcinogens such as AFB_1 and the heterocyclic amines within the diet or digestive system currently remains unknown. Given the relative strength of the complex between AFB_1 and CHL, and the presence of other porphyrinic compounds in the human diet, complex formation may play an important role in reducing the overall bioavailability of polycyclic planar carcinogens from the human diet, even if the extent of complexation is less than might be predicted by simple solution model measurements.

Additional mechanisms for CHL-mediated reduction of target organ carcinogen–DNA binding may involve localized CHL–carcinogen complexation, inhibition of carcinogen-activating enzymes, or degradation of ultimate carcinogens within the target cells (*15*, *28*). The kinetic data presented here suggested apparent noncompetitive inhibition by CHL for the enzymatic activation of AFB_1. Formally, this result would be expected if CHL interacts with substrate (AFB_1) as well as enzyme. However, additional kinetic analyses and a systematic analysis of CHL chromophore distribution in vivo are needed in order to more clearly define and evaluate the in vivo relevance of such additional inhibitory mechanisms.

Acknowledgment. We wish to thank Dr. Randy Larsen, Department of Chemistry, University of Hawaii, for assistance with the HyperChem software. This work was partially supported by Grant CA34732 from the National Cancer Institute, and by Center Grants ES03850 and ES00210 from the National Institute of Environmental Health Sciences. This is technical paper 10 576 from the Oregon Agricultural Experiment Station.

References

(1) Wattenberg, L. W. (1983) Inhibition of neoplasia by minor dietary constituents. *Cancer Res.* **43** (Suppl.), 2448–2453.
(2) Hayatsu, H., Arimoto, S., and Negishi T. (1988) Dietary inhibitors of mutagenesis and carcinogenesis. *Mutat. Res.* **202**, 429–446.
(3) Dragsted, L. O., Strube, M., and Larsen, J. C. (1993) Cancer-protective factors in fruits and vegetables: Biochemical and biological background. *Pharmacol. Toxicol.* **72** (Suppl. 1), 116–135.
(4) Dashwood, R. H., Breinholt, V., and Bailey, G. S. (1991) Chemopreventive properties of chlorophyllin: inhibition of aflatoxin-B_1 (AFB_1)–DNA binding *in vivo* and anti-mutagenic activity against AFB_1 and two heterocyclic amines in the Salmonella mutagenicity assay. *Carcinogenesis* **12**, 939–942.
(5) Breinholt, V., Hendricks, J., Pereira, C., Arbogast, D., and Bailey, G. (1995) Dietary chlorophyllin is a potent inhibitor of aflatoxin B^1 hepatocarcinogenesis in rainbow trout. *Cancer Res.* **55**, 57–62.
(6) Khachik, F., Beecher, G. R., and Whittaker, N. F. (1986) Separation, identification and quantification of the major carotenoid and chlorophyll constituents in extracts of several green vegetables by liquid chromatography. *J. Agric. Food Chem.* **34**, 603–616.
(7) Khalyfa, A., Kermasha, S., and Alli, I. (1992) Extraction, purification, and characterization of chlorophyll from spinach leaves. *J. Agric. Food Chem.* **40**, 215–220.
(8) Arimoto, S., Negishi, T., and Hayatsu, H. (1980) Inhibitory effect of hemin on the mutagenic activities of carcinogens. *Cancer Lett.* **11**, 29–33.
(9) Arimoto, S., and Hayatsu, H. (1989) Role of hemin in the inhibition of mutagenic activity of 3-amino-1-methyl-5H-pyrido-[4,3-b]indole (Trp-P-2) and other aminoazaarenes. *Mutat. Res.* **213**, 217–226.
(10) Dashwood, R. H., and Guo, D. (1992) Inhibition of 2-amino-3-methylimidazo[4,5-*f*]quinoline (IQ)–DNA binding by chlorophyllin: studies of enzyme inhibition and molecular complex formation. *Carcinogenesis* **13**, 1121–1126.
(11) Newmark, H. L. (1984) A hypothesis for dietary components as blocking agents of chemical carcinogenesis: Plant phenolics and pyrrole pigments. *Nutr. Cancer* **6**, 58–70.
(12) Newmark, H. L. (1987) Plant phenolics as inhibitors of mutational and precarcinogenic events. *Can. J. Physiol. Pharm.* **65**, 461–466.
(13) Negishi, T., Arimoto, S., Nishizaki, C., and Hayatsu, H. (1989) Inhibitory effect of chlorophyll on the genotoxicity of 3-amino-1-methyl-5H-pyrido[4,3-b]indole (Trp-P-2). *Carcinogenesis* **10**, 145–149.
(14) Katoh, Y., Nemoto, N., Tanaka, M., and Takayama, S. (1983) Inhibition of benzo[a]pyrene-induced mutagenesis in Chinese hamster V79 cells by hemin and related compounds. *Mutat. Res.* **121**, 153–157.
(15) Dashwood, R. H. (1992) Protection by chlorophyllin against the covalent binding of 2-amino-3-methylimidazo[4,5-*f*]quinoline (IQ) to rat liver DNA. *Carcinogenesis* **13**, 113–118.
(16) International Agency for Cancer Research (1993) *IARC Monographs on the Evaluation of the Carcinogenic Risk of Chemicals to Humans: Aflatoxins*, Vol. 56, pp 245–396, IRAC, Lyon, France.
(17) Sato, M., Fujimoto, I., Sakai, T., Aimoto, T., Kimura, R., and Murata, T. (1986) Effect of sodium copper chlorophyllin on lipid peroxidation. IX. On the antioxidative components in commercial preparations of sodium copper chlorophyllin. *Chem. Pharm. Bull.* **34**, 2428–2434.
(18) Shelnutt, J. A. (1984) Electronic structure of the porphyrin ring in an electrostatically bound π–π complex. Methylviologen–metalloporphyrin complexes. *J. Phys. Chem.* **88**, 6121–6127.
(19) Arimoto, S., Fukuoka, S., Itome, H. C., Nakano, H., Rai, H., and Hayatsu, H. (1993) Binding of polycyclic planar mutagens to chlorophyllin resulting in inhibition of the mutagenic activity. *Mutat. Res.* **287**, 293–305.
(20) Eisele, T. A., Bailey, G. S., and Nixon, J. E. (1983) The effect of indole-3-carbinol, an aflatoxin B_1 hepatocarcinoma inhibitor, and other indole analogs on the rainbow trout mixed function oxidase system. *Toxicol. Lett.* **19**, 133–138.
(21) Lowry, O. H., Rosebrough, N. J., Far, A. L., and Randall, R. J. (1951) Protein measurements with the Folin phenol reagent. *J. Biol. Chem.* **193**, 265–275.
(22) Burton, K. (1956) A study of the conditions and mechanisms of the diphenylamine reaction for the colorimetric estimation of deoxyribonucleic acid. *Biochem. J.* **62**, 315–322.
(23) Dashwood, R. H., Arbogast, D. N., Fong, A. T., Hendricks, J. D., and Bailey, G. S. (1988) Mechanisms of anticarcinogenesis by indole-3-carbinol: detailed *in vivo* DNA binding dose–response studies after dietary administration with aflatoxin B_1. *Carcinogenesis* **9**, 427–432.
(24) Monroe, D. H., and Eaton, D. L. (1987) Comparative effects of butylated hydroxyanisole on hepatic *in vivo* DNA-binding and *in vitro* biotransformation of aflatoxin B_1 in the rat and mouse. *Toxicol. Appl. Pharmacol.* **90**, 401–409.
(25) Christwell, C. D., and Schilt, A. A. (1975) New and improved techniques for applying the mole ratio method to the identification of weak complexes in solution. *Anal. Chem.* **47**, 1623–1629.
(26) Pohland, A. E., Cushmac, M. E., and Andrellos, P. J. (1968) Aflatoxin B_1 hemiacetal. *J. Assoc. Offic. Anal. Chem.* **51**, 907–910.
(27) Williams, D. E., and Buhler D. R. (1983) Purified form of cytochrome P-450 from rainbow trout with high activity toward conversion of aflatoxin B_1 to aflatoxin B_1-2,3-epoxide. *Cancer Res.* **43**, 4752–4756.
(28) Tachino, N., Guo, D., Dashwood, W. M., Yamane, S., Larsen, R., and Dashwood, R. H. (1994) Mechanisms in the in vitro antimutagenic action of chlorophyllin against benzo[a]pyrene: Studies of enzyme inhibition, molecular complex formation and degradation of the ultimate carcinogen. *Mutat. Res.* **308**, 191–302.

(29) Sato, M., Konagai, K., Kuwana, T., Kimura, R., and Murata, T. (1984) Effects of sodium copper chlorophyllin on lipid peroxidation. VII. Effects of its administration on the stability of rat liver lysosomes. *Chem. Pharm. Bull.* **32**, 2855–2858.
(30) Sato, M., Imai, K., Kimura, R., and Murata, T. (1984) Effect of sodium copper chlorophyllin on lipid peroxidation. VI. Effects of its administration on mitochondrial and microsomal lipid peroxidation in rat liver. *Chem. Pharm. Bull.* **32**, 712–722.
(31) Imai, K., Aimoto, T., Sato, M., Watanabe, K., Kimura, R., and Murato, T. (1986) Effects of sodium metallochlorophyllins on the activity and components of the microsomal drug-metabolizing enzyme system in rat liver. *Chem. Pharm. Bull.* **34**, 4287–4293.
(32) Oda, T., Yokono, O., Yoshida, A., Miyake, K., and Iino, S. (1971) On the successful treatment of pancreatitis. *Gastroenterol. Jpn.* **6**, 49–54.
(33) Wu, Z. L., Chen, J. K., Ong, T., Brockman, H. E., and Whong, W.-Z. (1994) Antitransforming activity of chlorophyllin against selected carcinogens and complex mixtures. *Teratog., Carcinog. Mutagen.* **14**, 75–81.
(34) Ghosh, A., Sen, S., Sharma, A., and Talukder, G. (1991) Inhibitions of clastogenic effects of cesium chloride in mice *in vivo* by chlorophyllin. *Toxicol. Lett.* **57**, 11–17.
(35) Ghosh, A., Sen, S., Sharma, A., and Talukder, G. (1991) Effect of chlorophyllin on mercury chloride-induced clastogenicity in mice. *Food Chem. Toxicol.* **29**, 777–779.
(36) Robins, E. W., and Nelson, R. L. (1989) Inhibition of 1,2-dimethylhydrazine-induced nuclear damage in rat colonic epithelium by chlorophyllin. *Anticancer Res.* **9**, 981–986.
(37) Whong, W., Stewart, J., Brockman, H. E., and Ong T. (1988) Comparative antimutagenicity of chlorophyllin and five other agents against aflatoxin B_1-induced reversion in *Salmonella typhimurium* TA98. *Teratog., Carcinog. Mutagen.* **8**, 215–224.

TX940131B